

## Efficient Propagation of Polarization from Laser Photons to Positrons through Compton Scattering and Electron-Positron Pair Creation

T. Omori,<sup>1</sup> M. Fukuda,<sup>2</sup> T. Hirose,<sup>3</sup> Y. Kurihara,<sup>1</sup> R. Kuroda,<sup>3,4</sup> M. Nomura,<sup>2</sup> A. Ohashi,<sup>5</sup> T. Okugi,<sup>1</sup> K. Sakaue,<sup>3</sup> T. Saito,<sup>3</sup> J. Urakawa,<sup>1</sup> M. Washio,<sup>3</sup> and I. Yamazaki<sup>3</sup>

<sup>1</sup>KEK: High Energy Accelerator Research Organization, Tsukuba-shi, Ibaraki 305-0801, Japan

<sup>2</sup>National Institute of Radiological Sciences, Chiba-shi, Chiba 263-8555, Japan

<sup>3</sup>Advanced Research Institute for Science and Engineering, Waseda University, Tokyo 169-8555, Japan

<sup>4</sup>National Institute of Advanced Industrial Science and Technology, Tsukuba-shi, Ibaraki 305-8568, Japan

<sup>5</sup>Department of Physics, Tokyo Metropolitan University, Hachioji-shi, Tokyo 192-0397, Japan

(Received 10 September 2005; published 24 March 2006)

We have demonstrated for the first time the production of highly polarized short-pulse positrons with a finite energy spread in accordance with a new scheme that consists of two-quantum processes, such as inverse Compton scattering and electron-positron pair creation. Using a circularly polarized laser beam of 532 nm scattered off a high-quality, 1.28 GeV electron beam, we have obtained polarized positrons with an intensity of  $2 \times 10^4 e^+$ /bunch. The magnitude of positron polarization has been determined to be  $73 \pm 15(\text{stat}) \pm 19(\text{syst})\%$  by means of a newly designed positron polarimeter.

DOI: 10.1103/PhysRevLett.96.114801

PACS numbers: 29.27.Hj, 41.75.Fr

**Introduction.**—A positron( $e^+$ ), the antiparticle of an electron( $e^-$ ), is created from pair creation by high-energy photons and can also be obtained from beta decays of specific radioisotopes. Concerning polarization, positrons emitted from beta decays are longitudinally polarized but are subject to a large energy spread, a wide angular distribution, low intensity, etc, such that those positrons are far from practical usage as an  $e^+$  beam. It is widely believed that one of the next-generation accelerators at the energy frontier will be an electron-positron linear collider, the International Linear Collider (ILC), where the polarized  $e^+$  beams should play significant roles in studying the standard model as well as discovering phenomena beyond the standard model.

In 1996 we proposed a novel method [1] for creating highly polarized  $e^+$  beams with a finite energy spread through electron-positron pair creation from longitudinally polarized  $\gamma$  rays that are generated from the inverse Compton scattering of circularly polarized laser-photons. Figure 1 is a schematic diagram of the proposed method where the helicity of a laser photon is +1 (right-handed,  $R$ ), for example. Figure 2(a) shows the energy dependence of the cross section of the inverse Compton scattering in which a right-handed polarized laser light of wavelength 532 nm scatters off a relativistic electron beam with an energy of 1.28 GeV. Note that the left-handed  $\gamma$  rays dominate in the energy close to the maximum energy of 56 MeV. When these left-handed  $\gamma$  rays hit on a thin metallic target, highly polarized positrons are generated in the high-energy part of the spectrum, as can be seen in Fig. 2(b). We therefore are able to accomplish the efficient propagation of the polarization from the laser photon to the positron via two-quantum processes.

We have pursued proof-of-principle studies with the help of extensive Monte Carlo simulations [2,3]. One of

the important steps is to establish the polarimetry for short-bunch  $\gamma$  rays and positrons with a time duration of a few tens of picoseconds (ps). Usually, the  $\gamma$ -ray polarization can be determined using spin-dependent Compton scatterings of  $\gamma$  rays on electrons in  $3d$  orbits in magnetized iron. Actually, in this experiment, the magnetized iron is a 100 mm long iron pole of an electromagnet (called the analyzer magnet hereafter). However, the electron-positron pair creation in the analyzer magnet causes considerably large backgrounds that become a serious obstacle to cleanly extracting the Compton process. Thus, the Compton process has to be selected by means of a coincidence method in which both the electrons and  $\gamma$  photons emerging at the Compton scattering should be simultaneously identified. Unfortunately, such a short-bunch width of the  $\gamma$ -ray beam, only a few tens of picoseconds, prevents us from applying the coincidence method.

We adopted a “transmission method” in which only the intensity of the transmitted  $\gamma$  rays,  $N_P$  for the parallel cases and  $N_A$  for the antiparallel cases, was measured at a

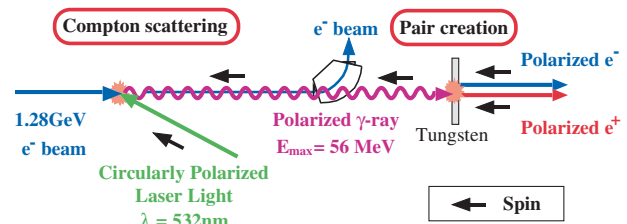


FIG. 1 (color). A fundamental scheme of polarized  $e^+$  production. Right-handed polarized laser photons are backscattered off relativistic electrons resulting in production of left-handed polarized  $\gamma$  rays in the forward direction (in the high-energy part of the spectrum). Pair creation of the  $\gamma$  rays through a tungsten plate generates left-handed positrons in the high-energy part.

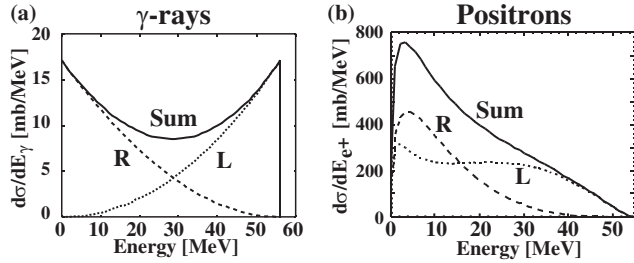


FIG. 2. (a) Differential cross section of the Compton scattering for right-handed polarized laser photons with wavelength of 532 nm backscattered off 1.28 GeV electrons as a function of the  $\gamma$ -ray energy. The dashed and dotted curves correspond to the helicities of +1 and -1 for the  $\gamma$  rays, respectively. (b) Differential cross section of the positron creation (electron-positron pair creation) in the thin tungsten target calculated using the  $\gamma$ -ray distribution given in Fig. 2(a). The dashed and dotted curves correspond to the helicities of +1 and -1 for the positrons.

position downstream of the analyzer magnet [4–6]. Here the parallel (antiparallel) case means that the spin of the  $\gamma$  rays and that of the electrons in the analyzer magnet are parallel (antiparallel) to each other. Hence the asymmetry is defined as  $A = (N_P - N_A)/(N_P + N_A)$ . The asymmetry is also the product of the polarization  $P$  and  $A_{MC}$ , the analyzing power estimated from the Monte Carlo simulation ( $A = PA_{MC}$ ). Because the transmitted  $\gamma$  rays are collimated to a narrow forward cone, whereas the Compton  $\gamma$  rays and the pair-created electrons and positrons as sources of background are emitted over a wide angular region, influence of such backgrounds is small enough that the transmission method can be applied to polarization measurements of  $\gamma$  rays with any time structure.

**Polarized positron production.**—A series of experiments has been conducted at the KEK-ATF, (Accelerator Test Facility) [7], consisting of an  $S$ -band linac and a damping ring, which provides high-quality 1.28 GeV  $e^-$  beams, with a typical beam intensity of  $1.8 \times 10^{10} e^-/\text{bunch}$ , a repetition rate of 3.12 Hz, a bunch length of 31 ps (rms), and an extremely small emittance. A mode lock Nd:YAG laser produces second-harmonic laser light with a wavelength of 532 nm, a pulse length of 110 ps (rms), and an average energy of 400 mJ/pulse. The laser light is converted into circularly polarized photons while passing through a quarter wave plate. The spot sizes in rms at the collision point are around 60  $\mu\text{m}$  (horizontal) and 40  $\mu\text{m}$  (vertical) for the  $e^-$  beam and 50  $\mu\text{m}$  for the round laser beam. The Compton backscattering of the polarized laser beam with the  $e^-$  beam generated polarized  $\gamma$  rays with a maximum energy of 56 MeV and a bunch length of 31 ps, being equal to the bunch length of the  $e^-$  beam.

Figure 3 shows an apparatus, called a Compton chamber, consisting of three cells together with the electron and laser beam lines. In order to achieve precise diagnoses for both beams, we installed screen monitors, a wire scanner and a

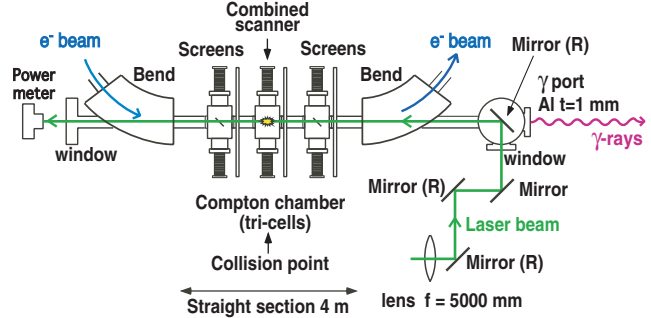


FIG. 3 (color). Experimental setup of the polarized  $\gamma$ -ray production system including the Compton chamber with three cells, the laser optics with three remotely controllable mirrors, and electron beam line. Laser-electron collisions take place at the central cell of the Compton chamber.

knife-edge scanner in the Compton chamber [8]. To observe the transverse position and the angle of both beams, the screen monitors were mounted in the central cell located at the collision point and in the side cells placed 265 mm away from the collision point. The wire scanner and the knife-edge scanner were set in the central cell. The wire scanner allows us to measure the  $e^-$  beam sizes at the collision point; and the knife-edge scanner determines the laser profile. The laser beam is transported to the collision point over a distance of about 10 m using six mirrors coated with a multilayer dielectric. The three mirrors can be remotely controlled to allow adjustment the position and angle of the laser beam at the collision point. Technical details on the production of polarized  $\gamma$  rays and the  $\gamma$ -ray polarimetry may be found in Ref. [8].

To maximize the collision probability of the laser photons and electrons, we optimized the laser optics as follows. The original laser beam was expanded to a spot size of 4.6 mm in rms and transported to the last lens with a relatively long focal-length, 5000 mm, resulting in a long collision distance of about 7 cm. Furthermore, to enable head-on collisions, the last mirror of 3 mm thickness was placed on the axis of the  $\gamma$  rays, as shown in Fig. 3. Note that loss of generated  $\gamma$  rays was negligible while passing through the mirror. The average number of  $\gamma$  rays generated in the inverse Compton process was  $2 \times 10^7/\text{bunch}$ . These  $\gamma$  rays were incident on a 1 mm thick tungsten plate for electron-positron pair creation. A separation magnet consisting of a pair of dipole magnets was installed after the tungsten plate, as shown in Fig. 4, to efficiently extract high-energy positrons that should have a high degree of polarization. We thus obtained  $2 \times 10^4 e^+/\text{bunch}$ . The numbers of  $\gamma$  rays and positrons were measured by an air Cherenkov counter and Si PIN photodiodes, respectively. While we did not measure the momentum of the positrons, according to simulation, the average energy of positrons is 36 MeV with rms width of 8 MeV.

**Positron polarimeter.**—Extending the transmission method employed in the  $\gamma$ -ray polarimetry [8], we have

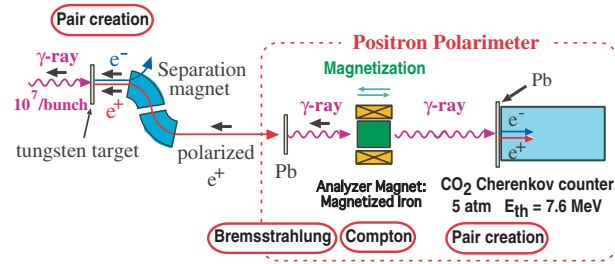


FIG. 4 (color). Schematic drawing for the  $e^+$  production apparatus and the polarimeter. Polarized  $\gamma$  rays are incident on a 1 mm thick tungsten plate resulting in electron-positron pair creation. The separation magnet installed after the tungsten plate efficiently extracts high-energy positrons, which generates circularly polarized  $\gamma$  rays through bremsstrahlung in the lead. The transmission of the  $\gamma$  rays can be measured with the  $\text{CO}_2$ -gas Cherenkov counter.

designed a  $e^+$  polarimeter whose schematic view is depicted in Fig. 4. The separated positrons hit a 6 mm thick lead converter, in which longitudinally polarized  $\gamma$  rays are again generated via the bremsstrahlung process from the positrons. The polarization of these  $\gamma$  rays can be measured by means of  $\gamma$ -ray polarimetry, the transmission method, which allows determination of the  $e^+$  polarization. The transmission  $T$  is defined as the number of transmitted  $\gamma$  rays normalized to the number of  $\gamma$  rays generated from inverse Compton scattering. In actual data treatment, an asymmetry is determined by flipping the polarity of the analyzer magnet. For a fixed state of the laser polarization, this corresponds a fixed state of the positron polarization, we measured the transmissions  $T_+$  and  $T_-$  for the magnetization direction being upstream and downstream of the positron flight direction, respectively. Thus the asymmetry,  $A$ , is given as  $A = (T_+ - T_-)/(T_+ + T_-)$ .

For checking the consistency of the whole system, measurements were carried out by reversing the laser polarization. Suppression of backgrounds from  $e^-$  beam halo interacting with the beam pipe and material surrounding it is critical to measurement as the asymmetry is very small ( $\sim 1\%$ ). Lead blocks were placed at appropriate locations along the beam line, and five-fold collimators were set between the collision point and the tungsten target to suppress the backgrounds. The  $e^+$  polarimeter was shielded with 20 cm thick iron walls in the front and 10 cm at the side. The photomultiplier of the  $\text{CO}_2$  Cherenkov counter was heavily shielded with lead blocks and was placed on the floor to escape from background produced by an  $e^-$  beam which was running at 1.2 m high. Also the gate width of the ADC to read the photomultiplier was minimized to 40 ns.

In order to maximize the spatial overlap between the  $e^-$  and laser beams, we precisely adjusted the position and angle of the laser beam using the three remotely controllable mirrors shown in Fig. 3. The collision timing was set

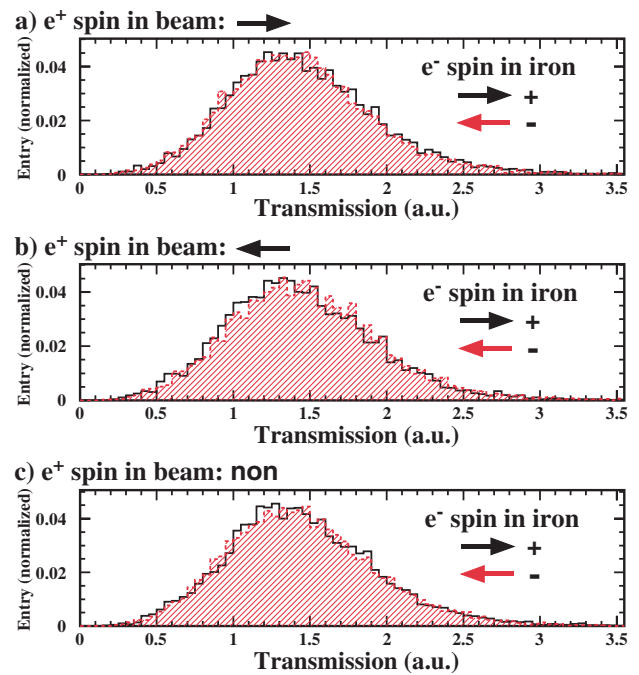


FIG. 5 (color). Measured asymmetries of polarized positrons for the different states of laser polarization (positron polarization). (a) Left-handed laser polarization (right-handed positron polarization). (b) Right-handed laser polarization (left-handed positron polarization). (c) Linear laser polarization (positrons are not longitudinally polarized). In each figure, the black line histogram and red-hatched histograms show distributions corresponding to magnetization directions being upstream (+) and downstream (-) of the positron flight direction.

such that the  $\gamma$ -ray signal after the Compton scatterings became largest by controlling the laser timing.

Taking into account all the elements of the polarimeter shown in Fig. 4, we performed various simulations to estimate the expected asymmetry with the help of the following simulation codes: CAIN [9] for Compton scattering of laser beams on  $e^-$  beams; GEANT3 [10] for electromagnetic interactions in a material; GRACE [11], particularly for spin-dependent electron-gamma interactions in the analyzer magnet; and POISSON [12] for iron magnetization.

*Results and conclusions.*—Figure 5(a) shows result of asymmetry measurement when laser polarization set to be left handed. The transmission distributions for the + and - magnetization directions are shown by black line and red-hatched histograms, respectively. The significant deviation between the two distributions can be observed, leading to an asymmetry of  $0.60 \pm 0.25\%$ . We conducted the same measurement by reversing the laser polarization and obtained an asymmetry of  $-1.18 \pm 0.27\%$  as given in Fig. 5(b). In order to check the consistency of the measurement, we also conducted the asymmetry measurement for linear laser polarization, which should correspond to zero longitudinal polarization of positrons: The results of

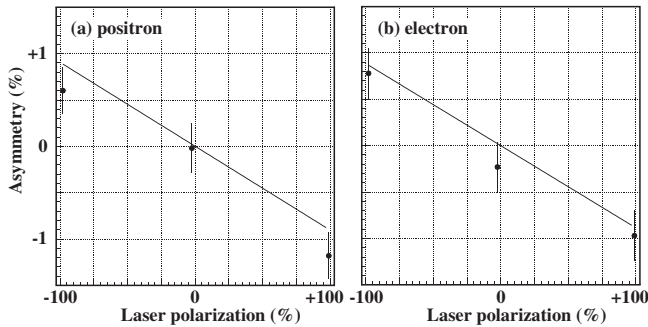


FIG. 6. Measured asymmetry as a function of the circular polarization of a laser beam. Straight lines are result of linear fitting with a constraint of passing the origin (0, 0); (a) result of the positron measurement, (b) result of the electron measurement. Note: When the direction of photon spin and the direction of its momentum is parallel, we call it right handed. When a laser beam is 100% right-handed polarized, we call it +100%.

this run are shown in Fig. 5(c), from which we obtained an asymmetry of  $-0.02 \pm 0.25\%$ , which is consistent with zero polarization of positrons. Here, all errors noted above are statistical ones. The results of asymmetry measurement corresponding to three laser polarization shown in Figs. 5(a)–5(c) are plotted in Fig. 6(a). As shown in Fig. 6(a), we fit a straight line to the data. In the fitting the line is constrained to pass through the origin (0, 0). Hence the absolute value of the slope is obtained to be  $0.90 \pm 0.18\%$  with a reduced  $\chi^2$  of 1.3. Here the error represents the fitting error and therefore it is essentially statistical. This slope corresponds to the positron asymmetry with 100% laser polarization. From this asymmetry, the magnitude of the positron polarization was calculated as  $73 \pm 15 \pm 19\%$ , where the first error is a statistical one (the fitting error) and the second error is systematic one which comes from the uncertainty in a Monte Carlo simulation. The measured value of the polarization is consistent with the value of 77% estimated by a Monte Carlo simulation.

For further confirmation, we also produced polarized electrons by reverting the polarity of the separation magnet (see Fig. 4) and performed polarization measurements. The measured asymmetries were  $0.78 \pm 0.27\%$  and  $-0.97 \pm 0.27\%$  for left-handed and right-handed laser polarization, respectively. And for the linear laser polarization, the asymmetry was measured to be  $-0.23 \pm 0.27\%$ . The results of electron measurements are plotted in Fig. 6(b) with result of linear fitting. The asymmetry calculated from the fitting is  $0.89 \pm 0.19\%$ , with reduced  $\chi^2$  of 0.55. The data of positron polarization and electron polarization are in agreement with each other.

The present results have demonstrated for the first time the viability of our proposed scheme, which is based on two-quantum processes, namely, inverse Compton scattering of circularly polarized laser light on high-quality elec-

tron beams and electron-positron pair creation. It has been verified that efficient propagation of the polarization to the positrons by imposing specific kinematical conditions, specially the selection of relatively high-energy positrons. Using a circularly polarized laser beam of 532 nm scattered off a high-quality 1.28 GeV electron beam, we have obtained polarized  $\gamma$  rays of  $2 \times 10^7$ /bunch and polarized positrons of  $2 \times 10^4$ /bunch. We have established positron polarimetry based on the so-called transmission method and have obtained a transmission asymmetry of  $0.90 \pm 0.18\%$  leading to a positron polarization of  $73 \pm 15(\text{stat}) \pm 19(\text{syst})\%$ . This value is in good agreement with the value of 77% derived from Monte Carlo simulations in which basic QED processes and beam parameters are involved. Various techniques developed in this study for finding the optimal condition for laser-electron beam collisions will be of great use to the development of extremely precise beam diagnoses required by future linear colliders or third-generation electron accelerators. The present results encourage the realization of polarized positron beam [13] for the future linear collider ILC.

We would like to thank all members of the ATF group for the operation of ATF accelerator. We also acknowledge Mr. K. Sugiyama, Dr. K. Dobashi, Dr. I. Sakai, Dr. T. Muto, Ms. A. Higurashi, Mr. T. Iimura, Mr. T. Aoki for their important past contributions in developing the experimental apparatus, the electron and laser beam optics, and the data analysis. This research was partially supported by a Grant-in-Aid for Scientific Research (B)11554010, (A)11694092, (C)10640294, by a research program of U.S.-Japan Cooperation in the Field of High-Energy Physics, and by Advanced Compact Accelerator Project of National Institute of Radiological Sciences.

- 
- [1] T. Okugi *et al.*, Jpn. J. Appl. Phys. **35**, 3677 (1996).
  - [2] T. Hirose *et al.*, Nucl. Instrum. Methods Phys. Res., Sect. A **455**, 15 (2000).
  - [3] I. Sakai *et al.*, Phys. Rev. ST Accel. Beams **6**, 091001 (2003).
  - [4] G. Culligan *et al.*, Nature (London) **180**, 751 (1957).
  - [5] M. Goldhaber *et al.*, Phys. Rev. **109**, 1015 (1958).
  - [6] P. C. Macq *et al.*, Phys. Rev. **112**, 2061 (1958).
  - [7] K. Kubo *et al.*, Phys. Rev. Lett. **88**, 194801 (2002).
  - [8] M. Fukuda *et al.*, Phys. Rev. Lett. **91**, 164801 (2003).
  - [9] K. Yokoya, CAIN, <http://www-acc-theory.kek.jp/members/caain/default.html>.
  - [10] Application Software Group, CN Division, CERN Program Library Long Writeup W5013.
  - [11] T. Ishikawa *et al.* (Minami-Tateya Collaboration), KEK Report No. 92-19, 199.
  - [12] POISSON SUPERFISH, Los Alamos National Laboratory Report No. LA-UR-96-1834.
  - [13] T. Omori *et al.*, Nucl. Instrum. Methods Phys. Res., Sect. A **500**, 232 (2003).